PROCEEDINGS OF THE SEVENTH INTERNATIONAL CONFERENCE ON COMPUTER METHODS AND ADVANCES IN GEOMECHANICS / CAIRNS / 6 - 10 MAY 1991

Computer Methods and Advances in Geomechanics

Edited by

G. BEER
CSIRO, Division of Geomechanics

J. R. BOOKER & J. P. CARTER
University of Sydney

OFFPRINT

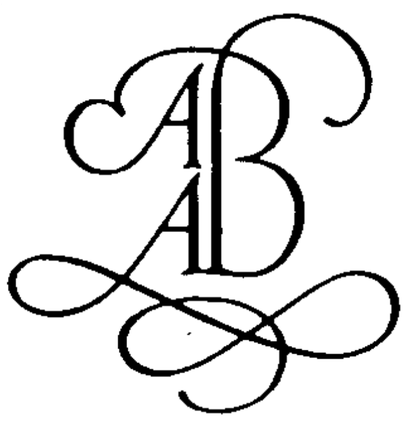

Published on behalf of the International Association for Computer Methods and Advances in Geomechanics by

A. A. BALKEMA / ROTTERDAM / BROOKFIELD / 1991

Computer Methods and Advances in Geomechanics, Beer, Booker & Carter (eds)
 ISBN 90 6191 189 3

Non-linear finite element analysis of safety factors

R. B. J. Brinkgreve
Delft University of Technology, Netherlands

H. L. Bakker
Public Works Department, Netherlands

ABSTRACT: In this paper a robust method is proposed to determine the safety factor of geotechnical constructions in finite element computations. The method is based on the reduction of the strength parameters of soil, the friction angle ϕ and the cohesion c. Three examples show the practical application of the method.

1 INTRODUCTION

In structural engineering a factor of safety is always defined as the ratio of the collapse load over the the working load. The same definition is adopted in foundation engineering, at least for footings and piles. For soil bodies such as road/river embankments and earthen dams the situation is different. Here the dominating load is not a direct external force, but most of the load comes from soil weight. Very cohesive soil bodies can be loaded to collapse by increasing gravity, either numerically or in centrifuge tests, but not when the strength is dominated by friction. Therefore other definitions of safety are common in soil mechanics. The usual soil mechanics definition of safety is:

$$\text{safety factor} = \frac{S}{S_c} = \frac{c + \sigma' \tan\phi}{c_c + \sigma' \tan\phi_c}$$

where S is the shear strength, further defined by the well known Mohr-Coulomb criterion. Note that c is the cohesion, ϕ is the friction angle and σ' is the normal pressure at the plane considered. Both c and ϕ are effective strength parameters and σ' is an effective stress. We use the subscript $_c$ to indicate critical strength parameters; just high enough to ensure equilibrium. Indeed, for $c=c_c$ and $\phi=\phi_c$ the safety factor becomes equal to unity. The above definition of safety coincides with the classical definition as used in slip circle analysis on the condition that we define:

$$c_c / \tan\phi_c = \alpha\, c / \tan\phi \qquad \text{with} \quad \alpha = 1$$

In this study the proportionality with α=1 will be retained in order to remain compatible to traditional slip circle analysis, but the method allows for other ratios of c_c and $\tan\phi_c$.

This study concentrates on the computation of the above safety factor by use of an elastic-plastic finite element method. In stead of the usual incrementation of loads, strength parameters will be decremented. This technique was first proposed by Zienkiewicz at al. (1975), but we make the procedure robust by adding an arc-length technique. A robust procedure was needed for implementing into the PLAXIS finite element package. Finally the potential of the method is demonstrated by considering a number of applications.

2 MOHR-COULOMB MODEL

Being interested in collapse loads rather than precise deformations, the elastic-plastic Mohr-Coulomb model is adopted. Hence

$$\dot{\underline{\sigma}} = \underline{D}\,(\,\dot{\underline{\varepsilon}} - \dot{\underline{\varepsilon}}^P) \quad , \qquad \dot{\underline{\varepsilon}}^P = \lambda \frac{\partial g}{\partial \underline{\sigma}}$$

where D is the elasticity matrix and

$$\lambda = \frac{1}{d} \frac{\partial f^T}{\partial \underline{\sigma}} \underline{D}\, \dot{\underline{\varepsilon}} \quad , \qquad d = \frac{\partial f^T}{\partial \underline{\sigma}} \underline{D} \frac{\partial g}{\partial \underline{\sigma}}$$

The symbols f and g are used to denote the yield function and the plastic potential function respectively. Considering planar deformations only, with the x-y-coordinates in the plane and the z-axis normal to the plane, we define

$$f = \tau - (c \cot\phi + \sigma) \sin\phi$$

$$g = \tau - \sigma \sin\psi$$

where

$$\tau^2 = \frac{1}{4}(\sigma_{xx} - \sigma_{yy})^2 + \sigma_{xy}^2 \quad , \quad \sigma = -\frac{1}{2}(\sigma_{xx} + \sigma_{yy})$$

For the sake of convenience, it is assumed that the out-of-plane stress σ_{zz} is in between the principal stresses $\sigma-\tau$ and $\sigma+\tau$.

3 IMPLICIT INTEGRATION

Finite element analyses involve finite increments of stress and strain rather than rates as considered above. Several integration rules can be applied to pass from rates to finite increments. One of the most popular ones, as first proposed by Vermeer (1979) and most recently by Borja & Lee (1990), is the implicit integration scheme. Here the direction of flow is considered to be fully determined by the state of stress at the end of a load increment. Denoting finite increments by the symbol Δ and t for time, we get

$$\Delta\underline{\varepsilon}^p = \int \lambda \frac{\partial g}{\partial \underline{\sigma}} dt = \frac{\partial g}{\partial \underline{\sigma}} \int \lambda \, dt = \frac{f^e}{d} \frac{\partial g}{\partial \underline{\sigma}}$$

where

$$f^e = f(\underline{\sigma}^* + \underline{D}\ \underline{\Delta\varepsilon})$$

where σ^* is the stress at the beginning of the load increment. Details are given by Vermeer & Van Langen (1989). Having defined the increment of plastic strain as a function of the total strain increment, it is easy to compute the stress increment from:

$$\Delta\underline{\sigma} = \underline{D}\ (\Delta\underline{\varepsilon} - \Delta\underline{\varepsilon}^p)$$

4 FINITE ELEMENT FORMULATION

We consider a soil body subject to constant gravity and constant external loads. These are equilibrated by a known stress field $\underline{\sigma}^o$. Hence, the finite element equilibrium conditions give:

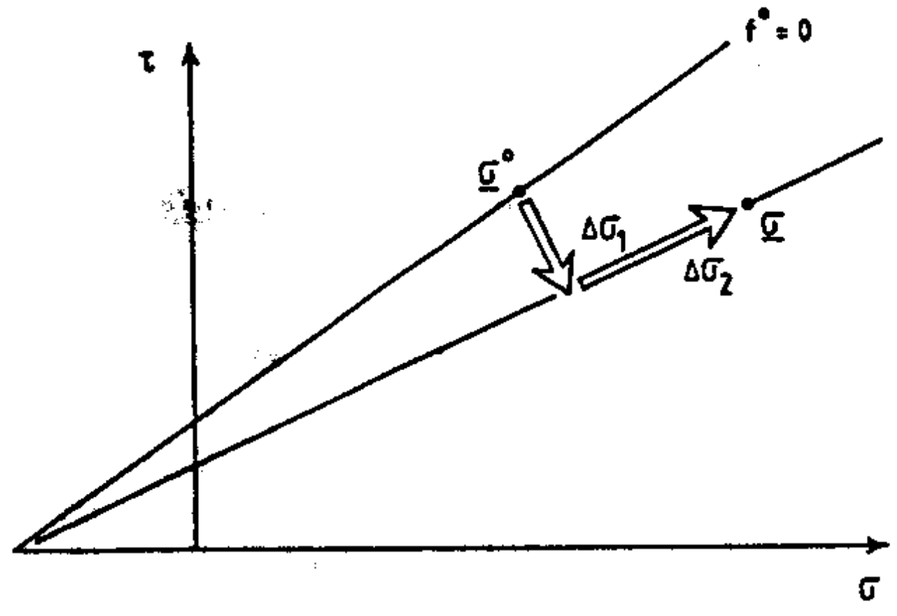

Fig. 1. Increments for strength-reduction

$$\int_V \underline{B}\ \underline{\sigma}^o\ dV = \underline{Q}^o \quad , \quad \int_V \underline{B}\ \underline{\sigma}\ dV = \underline{Q}^o$$

where both body forces and external loads are assembled in the vector $\underline{Q}$ for nodal forces. We now apply a decrement of the strength parameters, so that the yield locus rotates as indicated in Fig.1. Obviously, the new stresses $\underline{\sigma}$ (without superscript) will be at the new yield locus, at least for material points with stresses $\underline{\sigma}^o$ above this line. Let us now define

$$\underline{\sigma} \equiv \underline{\sigma}^o + \Delta\underline{\sigma}^1 + \Delta\underline{\sigma}^2 \quad , \quad \Delta\underline{\sigma}^2 \equiv \underline{D}\ (\Delta\underline{\varepsilon} - \Delta\underline{\varepsilon}^p)$$

where $\underline{\sigma}^o + \Delta\underline{\sigma}^1$ is the closest point projection of $\underline{\sigma}^o$ on the new yield surface. Substitution in the equilibrium equation, and using $\underline{\varepsilon} = \underline{B}\ \underline{u}$, gives:

$$\underline{K}\ \Delta\underline{u} = \underline{R}^o + \Delta\underline{R} + \underline{P}$$

where $\underline{K}$ is the elastic stiffness matrix and

$$\underline{R}^o = \underline{Q}^o - \int_V \underline{B}\ \underline{\sigma}^o\ dV = 0$$

$$\Delta\underline{R} = -\int_V \underline{B}\ \Delta\underline{\sigma}^1\ dV \quad , \quad \underline{P} = \int_V \underline{B}\ \underline{D}\ \Delta\underline{\varepsilon}^p\ dV$$

In practice $\underline{R}^o$ will not entirely vanish because of numerical procedures; separation from $\Delta\underline{R}$ is important for later formulation of an arc-length control procedure. $\underline{P}$ is a pseudo load vector, as used within an initial-stress iteration-procedure of the type:

$$K\ \Delta\underline{u}^{k+1} = \underline{R}^o + \Delta\underline{R} + \underline{P}^k,$$

$$\text{for } k=1,2,..k_{max} \quad \text{and } \underline{p}^1 = 0$$

We adopt an initial stress procedure since a tangent stiffness procedures tend to break down in the fully plastic range due to ill-conditioning.

5 INDIRECT DISPLACEMENT CONTROL

The above strength reduction procedure is is far from being robust. Indeed, by a step wise decrease of strength it is possible to approach collapse, but for some step the strength will be reduced too much, i.e. beyond critical, so that the iterative procedure will not converge to an equilibrium state of stress. In this manner the precise critical values of tanϕ and c are never obtained. Therefore indirect displacement control is needed, or in other words arc-length control (Rheinboldt & Riks, 1986). Within this approach we add a load multiplier β, and obviously an extra scalar equation for solving β. The system of iteration equations is

$$\underline{K}\ \Delta\underline{u}^k = \underline{R}^o + \beta^k \Delta\underline{R} + \underline{P}^{k-1}$$
$$\Delta\underline{u}_o^T\ \Delta\underline{u}^k = \Delta\underline{u}_o^T\ \Delta\underline{u}_o$$

The subscript o is used to denote results from the previous load step. Instead of the node displacement vector of the previous step, other vectors can be used to obtain a linear scalar equation for β. Similarly non-linear equations are feasible.

6 STABILITY OF RIVER EMBANKMENT

The first practical application involves a river embankment in the tidal zone. The slope has a horizontal length of 10 m and a height of 5 m, so the ratio is 1:2. The most dangerous situation for a embankment is at the onset of low tide. The waterlevel outside the embankment is already low, but the phreatic level in the embankment is still high. The situation, which is modelled is shown in Fig. 2. We consider a homogeneous soil with material properties as indicated in Table 1.

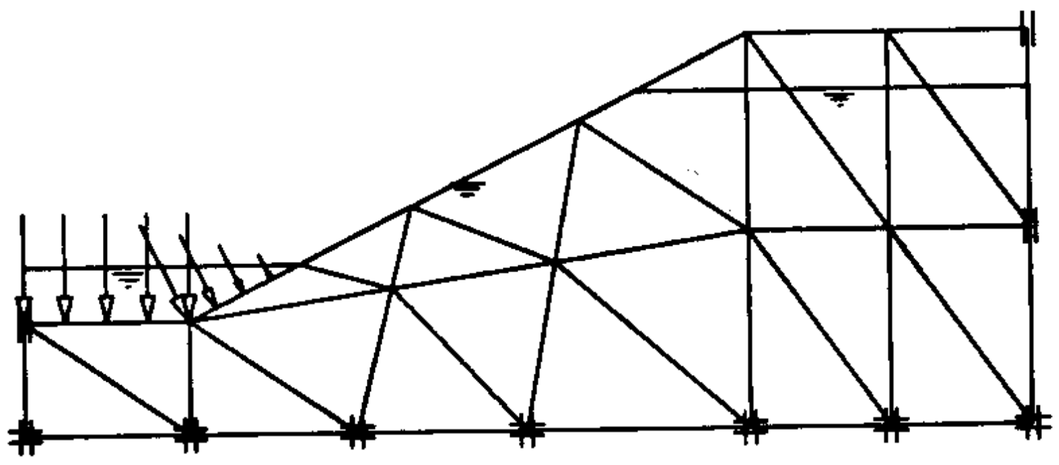

Fig. 2. River embankment at low tide

Table 1. Soil properties for embankment

Parameter	Symbol	Value
Dry weight	γ_d	16.0 kN/m^3
Wet weight	γ_w	20.0 kN/m^3
Friction angle	ϕ	30.0 $^\circ$
Cohesion	c	5.0 kPa
Shear modulus	G	1000 kPa
Poisson's ratio	ν	0.3

In the first part of the analysis we apply the soil weight to introduce the stresses for the situation of Fig. 2. Some of the Gaussian integration points appear to be in plastic state already, but the embankment has not collapsed at all.

In the second part of the calculation we want to analyze the safety of the construction. Therefore we apply ten steps in which the strength parameters of the soil are stepwise reduced, according to the theory as described before. When further reduction of the strength parameters in not possible anymore, the construction has collapsed and the safety factor is obtained. Fig. 3 shows the computed strength-displacement curve for the crest point of the embankment The value of the safety factor for this particular problem appears to be 1.20.

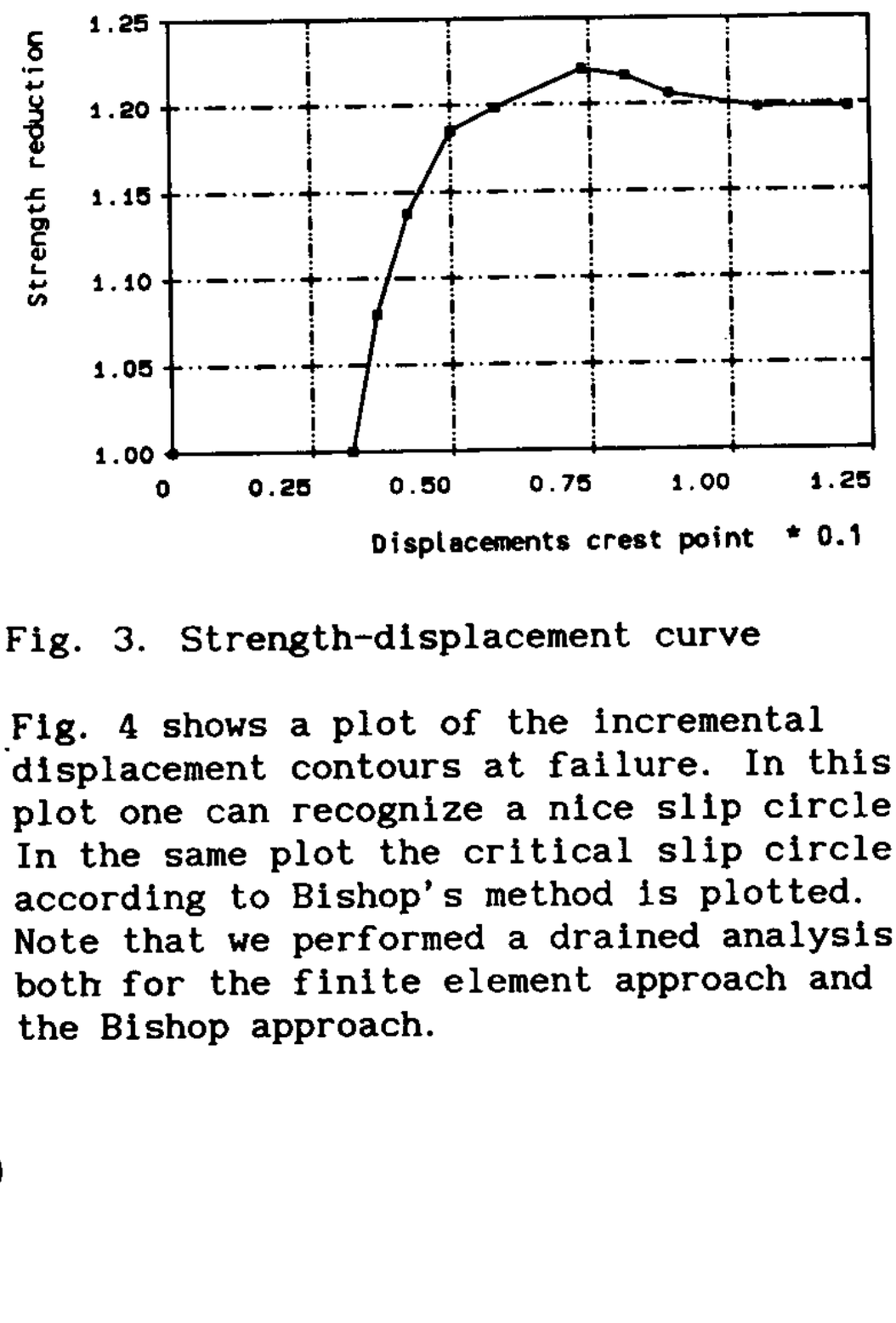

Fig. 3. Strength-displacement curve

Fig. 4 shows a plot of the incremental displacement contours at failure. In this plot one can recognize a nice slip circle. In the same plot the critical slip circle according to Bishop's method is plotted. Note that we performed a drained analysis both for the finite element approach and the Bishop approach.

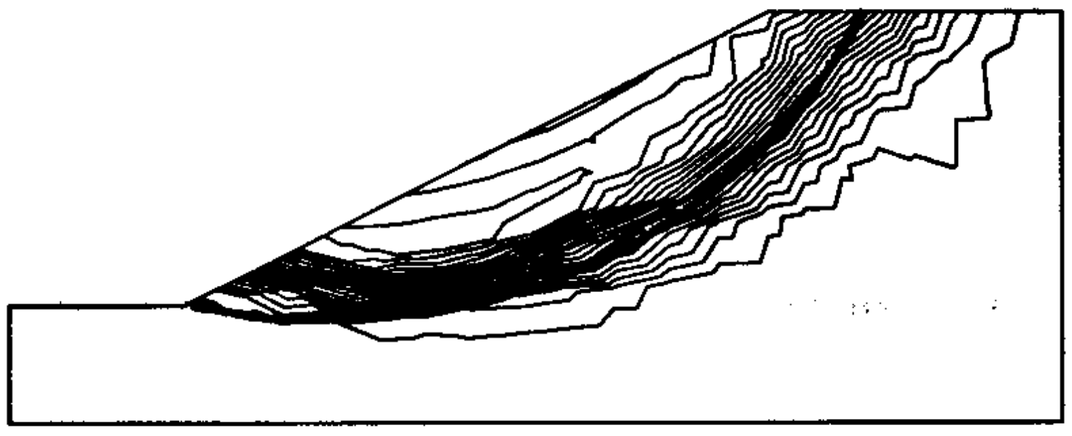

Fig. 4. Incremental displacement contours

Whilst the positions of the slip circles are somewhat different, the safety factor in both Bishop's method and the finite element calculation is exactly the same. This gives some validation of the proposed method. It might now be concluded that the calculation of the safety factor in finite element codes has no advantage in comparison with conventional methods. In this simple case this happens to be true, but the finite element method will also detect non-circular slip surfaces and associated factors of safety. The next examples will show that in general the finite element calculation of the safety factor gives information that cannot be obtained with conventional methods.

7 STABILITY OF A SHEET-PILE WALL

For the second application we consider the safety of an excavated building trench. The excavation depth is 21 m. The soil is supported by 32 m long sheet-pile walls, which are strutted at the top. During the excavation of the soil the water table remains at a constant level, both inside and outside the trench. Fig. 5 shows the finite element mesh of the trench. Special line elements, as available in the PLAXIS computer code, are used to model the sheet-pile wall (Bakker & Brinkgreve, 1990). The dashed lines in Fig. 5 indicate joint elements to model reduced friction at the soil-structure interface (Van Langen & Vermeer, 1990).

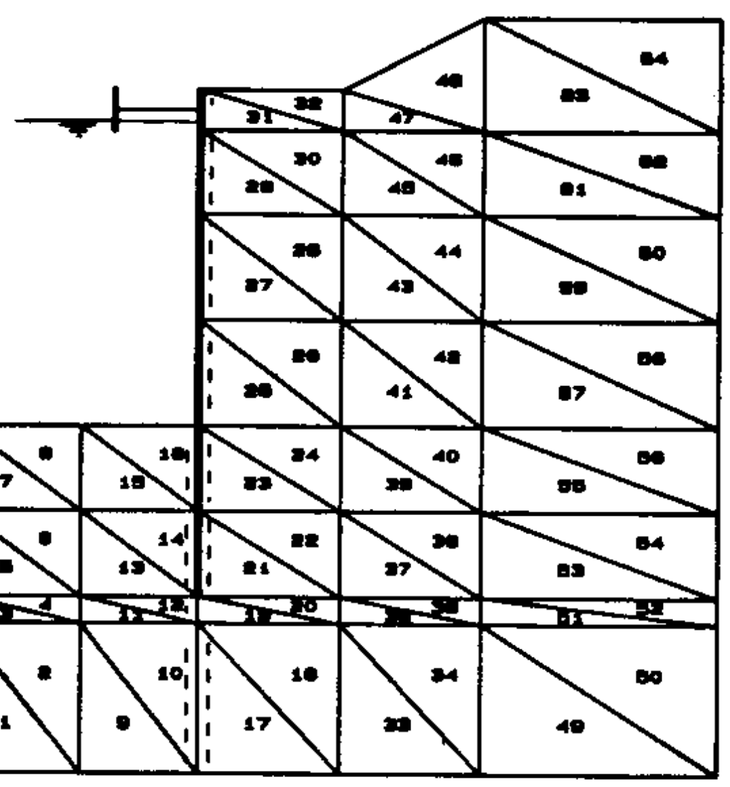

Fig. 5. Mesh for building trench

The soil is mostly fine silty sand with some clay layers. In fact it consists of 7 layers, which correspond to the element layers in the mesh of Fig 5. The material properties for each layer are given in Table 2. Layer No. 1 is the top layer and layer No. 7 is the lowest layer. For the sheet-pile wall and the strut we used:

$EI_{sheet} = 1.65 \times 10^6$ kNm^2/m

$EA_{sheet} = 8.04 \times 10^6$ kN/m

$EA_{strut} / L = 1.28 \times 10^5$ kN/m^2

Table 2. Properties for different layers

Layer	γ_d kN/m^3	γ_w kN/m^3	ϕ °	c kPa	G kPa
1	18.0	20.0	30.0	1.0	6000
2	16.0	16.0	25.0	8.0	3000
3		20.0	32.5	0.0	6000
4		20.0	32.5	0.0	8000
5		20.0	32.5	0.0	25000
6		18.0	27.5	4.0	9500
7		20.0	32.5	0.0	15000

The soil which is to be excavated, is modelled by external loads: horizontal tractions simulating the horizontal stresses at the sheet-pile wall and vertical tractions simulating the vertical stresses at the bottom of the trench.

The calculation consists of 3 parts. The first part is the introduction of the initial stresses including the tractions on the sheet-pile wall and the trench bottom.

The second part is the excavation of the trench by stepwise removing the external loads. Bending moments and strut forces occur in this part of the calculation. There is a stress reduction directly behind the sheet-pile wall mainly due to arching (Bakker & Brinkgreve, 1990). The extreme horizontal displacement of the sheet-pile wall is about 100 mm. The extreme bending moment amounts 2100 kNm/m and the strut force is 500 kN/m. Fig. 6 shows a plot of the incremental displacement contours at service state. A concentration of contour lines can be regarded as the initialisation of a shear band.

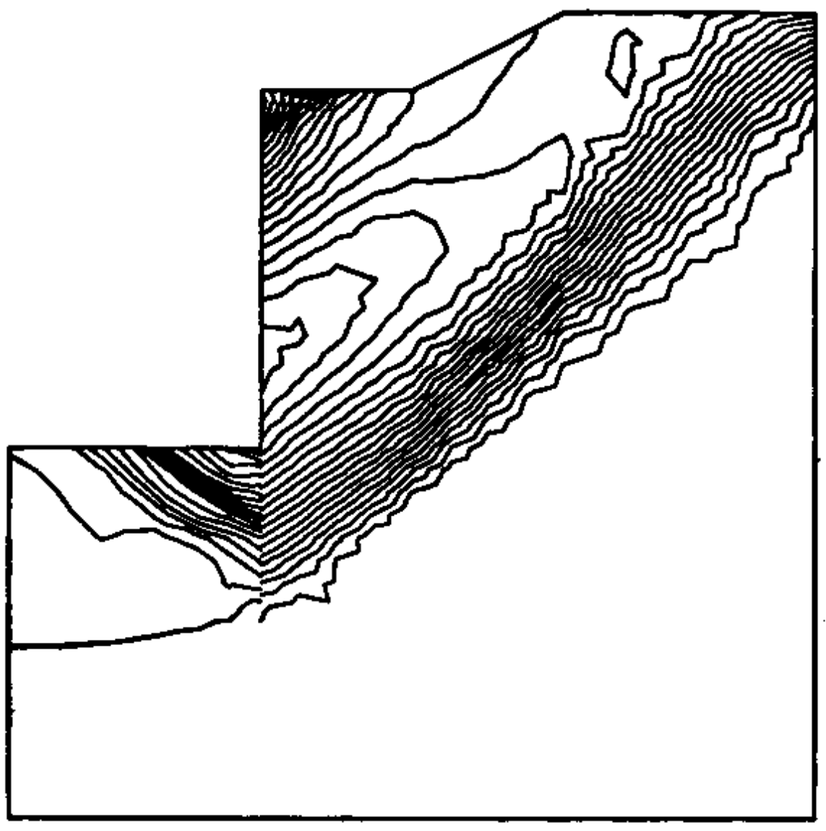

Fig. 6. Velocity contours at service state

The third part of the calculation is the determination of the safety factor by means of strength reduction. According to this calculation, the safety factor appears to be 1.65. The development of the bending moments during this calculation part is remarkable, as the clasping moment disappears and the sheet-pile wall tends to behave like a beam on two supports (Bakker & Brinkgreve, 1991).

Fig. 7 shows a plot of the incremental displacement contours at collapse. This plot visualizes a slip line going from the right-hand top, underneath the sheet-pile wall to the middle of the trench bottom. In comparison with the service state the slip line has moved drastically downwards.

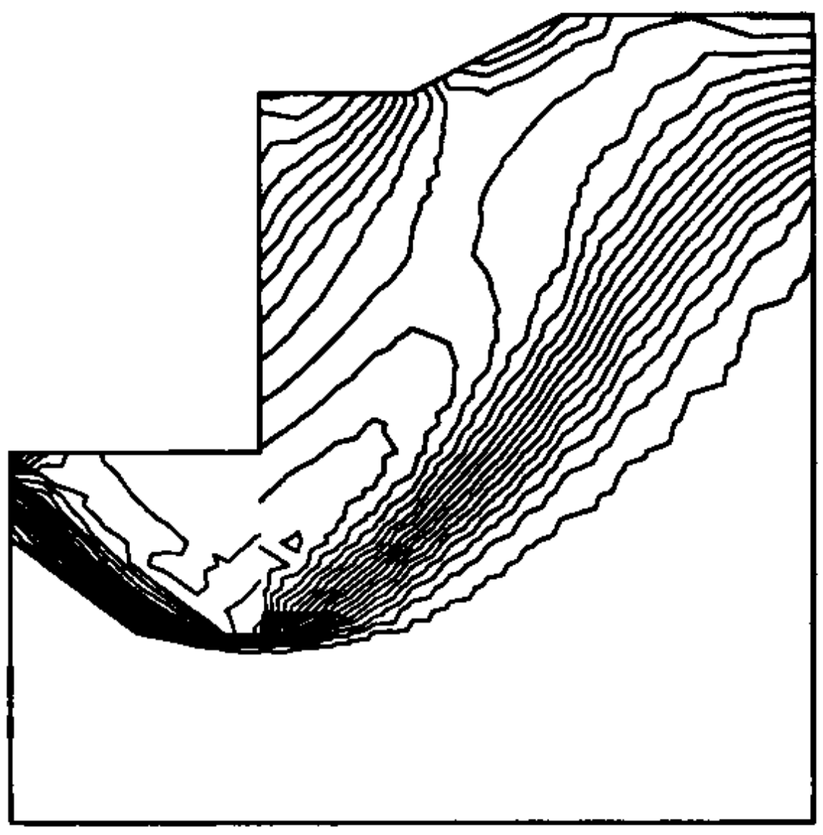

Fig. 7. Velocity contours at failure

8 EMBANKMENT STABILITY WITH GEOTEXTILE

The third application involves the safety of a road embankment. The embankment has a height of 6 m. In this example two situations are modelled: Firstly an ordinary case where the embankment is build just on top of the underground and secondly with the addition of a geotextile underneath the embankment. The situation is shown in Fig. 8.

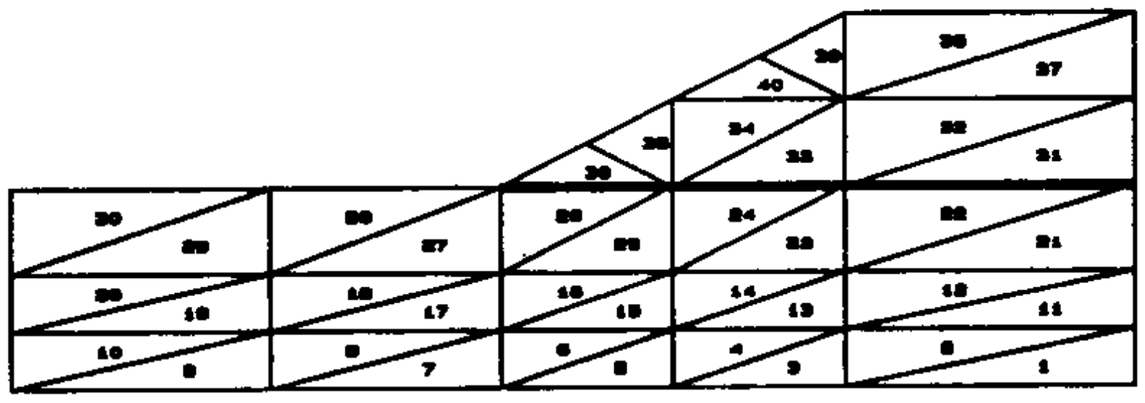

Fig. 8. Geometry of road embankment

The soil consists of four layers. The top layer is the embankment fill material. The underground consists of two clay layers with a layer of soft peat in between. The soil properties are given in Table 3.

Table 3. Properties for different layers

Layer	γ_d kN/m^3	γ_w kN/m^3	ϕ °	c kPa	G kPa	K_0
1	18.0	18.0	25.0	2.0	500	
2	18.0	18.0	24.0	5.0	500	0.60
3	11.0	11.0	15.0	2.0	250	0.75
4	18.0	18.0	24.0	5.0	500	0.60

Again the analysis consists of 3 parts. The first part is the introduction of the initial stresses in the underground. As the underground is horizontal the initial stresses can directly be derived from the soil weight and the K_0-values given in Table 3.

The second part of the calculation is the building of the embankment. At the end of this part the top of the embankment shows a settlement of 68 cm (without geotextile) and 66 cm (with geotextile). The geotextile seems to have little influence so far.

The third part is the calculation of the safety factor. Now the differences between both situations are much more apparent. In the case without geotextile the safety factor is less than 1.20 while in the case with geotextile the safety factor is over 1.30. In practice, only the latter situation is acceptable.

The difference in safety factor between the two situations is due to the fact that the failure mechanisms are completely different. Fig. 9 and 10 show plots of the incremental displacement contours of both situations. In the first case the failure mechanism is a slip circle going through the soft peat layer. In the second case the same mechanism is initially developed, but this is resisted by the geotextile. Collapse finally occurs in the embankment itself.

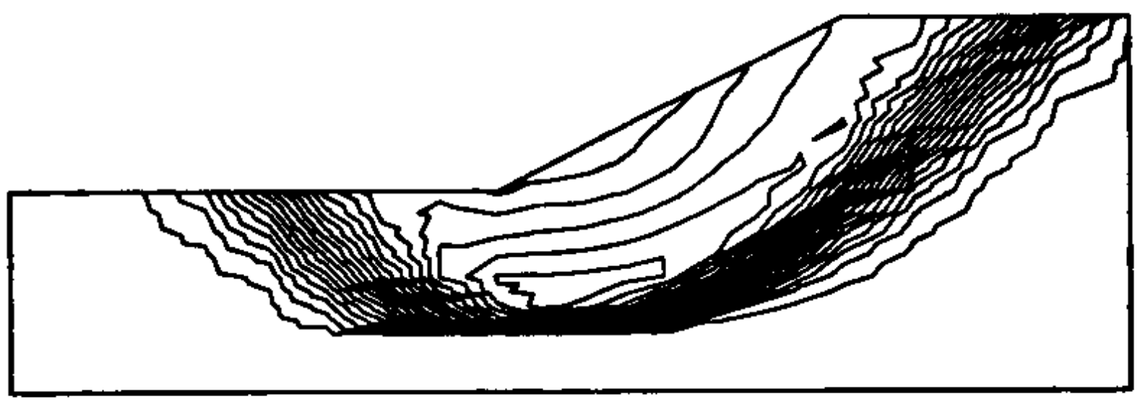

Fig.9. Velocity contours without geotextile

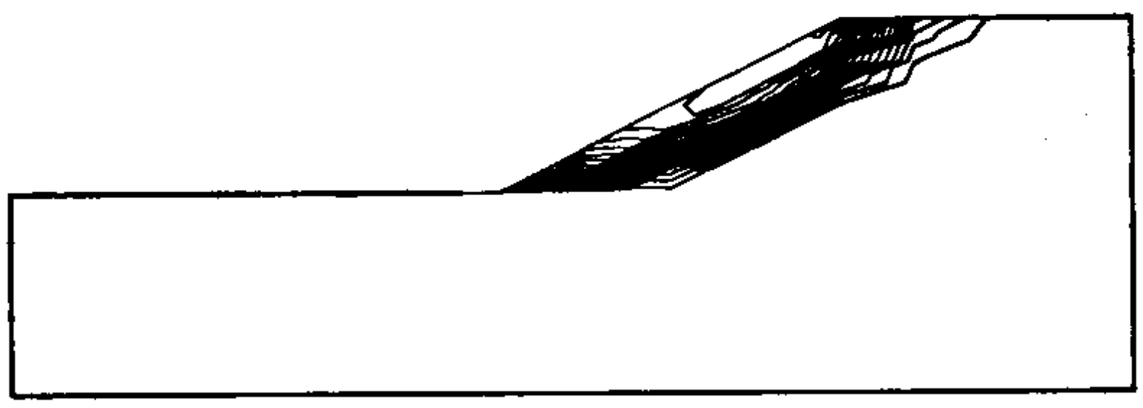

Fig. 10. Velocity contours with geotextile

Considering the results it would seem that geotextiles have an effect on stability rather than on deformation, but this will depend on the relative stiffness of the geotextile. For the present application we used EA = 2500 kN/m.

9 CONCLUDING REMARKS

The proposed finite element method for the determination of the safety factor by means of strength reduction gives results which agree well with those from Bishop's slip-circle method, at least for simple situations when a circular surface occurs.

The advantage of the method in comparison with conventional methods is that it even deals with the most complex kind of geotechnical constructions. Besides one does not have to predefine the failure mechanism.

Arc-length control makes the procedure robust since failure need not be associate with a non-converging iterative procedure. Moreover the arc-length procedure gives th full strength-displacement curves beyond possible peaks.

REFERENCES

Bakker, K.J. & Brinkgreve, R.B.J. 1990. The use of hybrid beam elements to model sheet-pile behaviour in two dimensional deformation analysis. In Proc. II Eur. Spec. Conf. on Num. Meth. in Geotech. Eng., p.559-571. Santander, CEDEX

Bakker, K.J. & Brinkgreve, R.B.J. 1991. Deformation analysis of a sheet-pile wall, using a two dimensional model. In Proc. X Eur. Conf. on Soil Mech. and Foundation Eng., Florence

Borja, R.I. & Lee, S.R. 1990. Cam-Clay plasticity, Part I: Implicit integration of elasto-plastic constitutive relations. In Comp. Meth. in Appl. Mech. and Eng, Vol 78, p.49-72

Rheinboldt, W.C. & Riks, E. 1986. Solution techniques for non-linear finite elements equations. In State-of-the-art surveys on finite element techniques, p.183-223. New York, Appl. Mech. Div. of ASME

Van Langen, H. & Vermeer, P.A. 1990. Finite element analysis of a pile penetration problem in clay. In Proc. II Eur. Spec. Conf. on Num. Meth. in Geotech. Eng., p.519-527., Santander, CEDEX

Vermeer, P.A. 1979. A modified initial strain method for plasticity problems. In Proc. III Int. Conf. on Num. Meth. in Geomech., p.377-387. Rotterdam, Balkema

Vermeer, P.A. & Van Langen, H. 1989. Soil collapse computations with finite elements. In Ingenieur-Archiv 59, p. 221-236

Zienkiewicz, O.C., Humpheson, C. & Lewis, R.W. 1975. Associated and non-associated visco-plasticity and plasticity in soil mechanics. Géotechnique 25, No. 4, p.671-689

Beer, G., J.R. Booker & J.P.Carter (eds.) 90 6191 189 3
Computer methods and advances in geomechanics – *Proceedings of the seventh international conference, Cairns, 6 – 10 May 1991*
1991, 25 cm, c.2000 pp., 3 vols., Hfl.385 / $210.00 / £122
Computer methods have become a powerful tool for solving problems in geomechanics & geotechnology. For example, in mining & civil engineering these methods have lead to improvements in design and are now applied to such diverse problems as rock mechanics, geophysics, geological engineering, ice mechanics, blasting & environmental geotechnology. The proceedings present the latest international research on the application of numerical methods to problems in geomechanics & on advances in constitutive modelling of geomaterials. In addition, new measurement & monitoring techniques & analytical methods are presented. Topics range from environmental to resource geotechnology including rock mechanics, geophysics, geological engineering, blasting, flow problems & more. Significant contributions are included on CAD/expert systems, groundwater geomechanics, back analysis & experimental studies.

FROM THE SAME PUBLISHER:

Swoboda, G. (ed.) 90 6191 809 X
Numerical methods in geomechanics: Innsbruck 1988
Proceedings of the sixth international conference, Innsbruck, 11 – 15 April 1988
1988–89, 25 cm, 2378 pp., 4 vols, Hfl.450 / $250.00 / £142
Main lectures; Numerical techniques & programming; Constitutive laws of geotechnical materials; Flow & consolidation; Ice mechanics; Rock hydraulics; Modeling of joints, interfaces & discontinuum; Modeling of infinite domains; Soil-structure interaction, piles; Earth structures, slopes, dams, embankments; Tunnels & underground openings; Dynamic & earthquake engineering problems, blasting; Mining applications; Interpretation of field measurements, back analysis; Microcomputers; Cad, mesh generation, software.

Dungar, R. & J.Studer (eds.) 90 6191 518 X
Geomechanical modelling in engineering practice
1986, 25 cm, 409 pp., Hfl.185 / $100.00 / £58
The key to successful solution of problems by the finite element method lies in the choice of appropriate numerical models & their associated parameters for geological media. 16 invited contributions from wellknown authorities from USA, UK, Switzerland, Japan & Canada on: Basic concepts; Numerical modelling of selected engineering problems; Specific numerical models & parameters evaluation.

Kolkman, P.A., J.Lindenberg & K.W.Pilarczyk (eds.)
90 6191 815 4
Modelling soil-water-structure interactions – SOWAS 88 – *Proceedings of the international symposium, Delft, 29.08–02.09.1988*
1988, 25 cm, 514 pp., Hfl.150 / $85.00 / £47
Soil-water-structure interactions; Wave and current induced behaviour of the seabottom; Local scour; Behaviour and stability of block revetments and filter layers; Wave impact loads and behaviour of asphalt revetments; Piles, platforms, piers and gravity structures; Sand suppletion processes and flow slides; Breakwaters, dams and walls. Miscellaneous.

Balasubramaniam, A.S., et al. (eds.) 90 6191 864 2
Computer and physical modelling in geotechnical engineering
Proceedings of the international symposium, Bangkok, 3–6 December 1986
1989, 25 cm, 550 pp., Hfl.190 / $105.00 / £60
Stability of natural & man made slopes; Design & design of foundations; Underground openings & excavations; Computer controlled testing & investigation of soils; Data acquisition & management in geotechnical engineering; Computer aided solutions for some special problems in engineering. 47 papers.

Ervin, M.C. (ed.) 90 6191 506 6
In-situ testing for geotechnical investigations – *Extension course, Sydney, May–June 1983*
1983, 25 cm, 140 pp., Hfl.100 / $55.00 / £32
An introduction to new developments, methods & applications of in-situ testing. 9 papers by Australian practising engineers & university lecturers. Editor: Coffey & Partners, Melbourne.

Alemayehu Teferra & Edgar Schultze 90 6191 804 9
Formulae, charts and tables in the areas of soil mechanics and foundation engineering– *Stresses in soils*
Formeln, Tafeln und Tabellen aus dem Gebiet Grundbau und Bodenmechanik – *Bodenspannungen*
1988, 25 cm, 300 pp., Hfl.95 / $50.00 / £30
This handbook is the result of many years of arduous work of systematically collecting the scattered scientific literature that is highly valuable to students and practicing engineers in the fields of soil mechanics and foundation engineering. The merit of the handbook lies not only in the compilation of important information that is normally not easily accessible to students and practicing engineers, but also in the provision of adequate illustrative examples that will facilitate the application of the formulae, charts and tables. In order to give the user the additional possibility to refer to the original works, references are given at the end of each topic. Elastic-isotropic half-space (Surface; Loads in half-space); Two layers – Vertical surface loading (Point loads; Line loads; Strip loading; Uniformly distributed rectangular loads; Axial symmetric loads; Loading with any shape; Stresses at interface); Multiple layers (Stresses at interfaces; Circular uniform loading). Authors: Addis Ababa University & German Academic Exchange.

Joshi, R.C. & F.J.Griffiths (eds.) 90 6191 707 7
Prediction and performance in geotechnical engineering – *Proceedings of an international symposium on prediction and performance in geotechnical engineering, Calgary, 17–19 June 1987*
1987, 25 cm, 464 pp., Hfl.150 / $85.00 / £47
Invited papers; Prediction & performance of pile foundations; Soil improvement; General prediction & performance of soils, unique soils, retaining structure behaviour & tunnels; Environmental geotechnology; Triaxial testing of soils; Centrifuge model testing; Risk analysis. 51 papers

Spencer, A.J.M. (ed.) 90 6191 682 8
Continuum models of discrete systems – *Proceedings of the fifth international symposium, Nottingham, 14–20 July 1985*
1987, 25 cm, 248 pp., Hfl.145 / $80.00 / £46
Recent developments in the study of material behavior, with particular emphasis on the difficult but important problems of relating behavior on the microscopic scale to that on the macroscopic scale. Authors were specially invited. 29 papers.

All books available from your bookseller or directly from the publisher:
A.A.Balkema Publishers, P.O.Box 1675, Rotterdam, Netherlands
For USA & Canada: A.A.Balkema Publishers, Old Post Rd, Brookfield, VT, USA